

Article

Role of Carnitine Acetyl Transferase in Regulation of Nitric Oxide Signaling in Pulmonary Arterial Endothelial Cells

Shruti Sharma *, Xutong Sun, Saurabh Agarwal, Ruslan Rafikov, Sridevi Dasarathy, Sanjiv Kumar and Stephen M. Black *

Pulmonary Vascular Disease Program, Vascular Biology Center, 1459 Laney Walker Blvd, Georgia Health Sciences University, Augusta, GA 30912, USA; E-Mails: xsun@georgiahealth.edu (X.S.); saggarwal@georgiahealth.edu (S.A.); rrafikov@georgiahealth.edu (R.R.); sdasarathy@georgiahealth.edu (S.D.); skumar@georgiahealth.edu (S.K.)

* Authors to whom correspondence should be addressed;

E-Mails: shsharma@georgiahealth.edu (S.S.); sblack@georgiahealth.edu (S.M.B.);

Tel.: +1-706-721-7860 (S.M.B.); Fax: +1-706-721-9799 (S.M.B.).

Received: 16 October 2012; in revised form: 26 November 2012 / Accepted: 30 November 2012 /

Published: 21 December 2012

Abstract: Congenital heart defects with increased pulmonary blood flow (PBF) result in pulmonary endothelial dysfunction that is dependent, at least in part, on decreases in nitric oxide (NO) signaling. Utilizing a lamb model with left-to-right shunting of blood and increased PBF that mimics the human disease, we have recently shown that a disruption in carnitine homeostasis, due to a decreased carnitine acetyl transferase (CrAT) activity, correlates with decreased bioavailable NO. Thus, we undertook this study to test the hypothesis that the CrAT enzyme plays a major role in regulating NO signaling through its effect on mitochondrial function. We utilized the siRNA gene knockdown approach to mimic the effect of decreased CrAT activity in pulmonary arterial endothelial cells (PAEC). Our data indicate that silencing the CrAT gene disrupted cellular carnitine homeostasis, reduced the expression of mitochondrial superoxide dismutase and resulted in an increase in oxidative stress within the mitochondrion. CrAT gene silencing also disrupted mitochondrial bioenergetics resulting in reduced ATP generation and decreased NO signaling secondary to a reduction in eNOS/Hsp90 interactions. Thus, this study links the disruption of carnitine homeostasis to the loss of NO signaling observed in children with CHD. Preserving carnitine homeostasis may have important clinical implications that warrant further investigation.

Keywords: carnitine acetyl transferase; superoxide dismutase; nitric oxide; peroxynitrite; endothelial nitric oxide synthase

1. Introduction

Children with congenital heart defects (CHD) that result in increased pulmonary blood flow (PBF) develop early and progressive alterations in pulmonary vascular function that cause significant morbidity [1]. The mechanisms involved in this pulmonary vascular disease are not fully understood, however, endothelial injury is thought to be an early hallmark [2,3]. Compelling evidence suggests that impaired NO signaling and oxidative stress play a key role in these events [4].

Oxidative and nitrative stress occurs when generation of reactive oxygen (ROS)- or nitrogen (RNS)-species overwhelms the cells natural antioxidant defenses, resulting in cellular damage and impaired function. Four enzyme systems are thought to predominate in vascular endothelial ROS generation: NADPH oxidase, xanthine oxidase, uncoupled eNOS and mitochondrial electron leakage. Whereas, the former three have been extensively studied, the role of mitochondrial derived ROS in the vascular endothelium has received less attention [5]. Mitochondria, through oxidative phosphorylation, are considered the major source of ROS in most mammalian cells. At the same time, mitochondria are potential targets of ROS action. Thus, increased ROS can damage DNA, proteins and lipids within the mitochondria, leading to alterations in the respiratory chain resulting in decreased energy production and a further increase in ROS generation (“ROS-induced ROS release”) [6,7]. In recent years, mitochondrial dysfunction has been acknowledged as a critical event in numerous pathologic conditions associated with oxidative stress, including diabetes mellitus, chronic renal failure, and neurodegenerative or cardiovascular diseases [5,8–10], and different antioxidants are being explored as potential therapeutic tools [11–13]. However, the contribution of the mitochondria to the pathogenesis of pulmonary vascular disease has been less well studied.

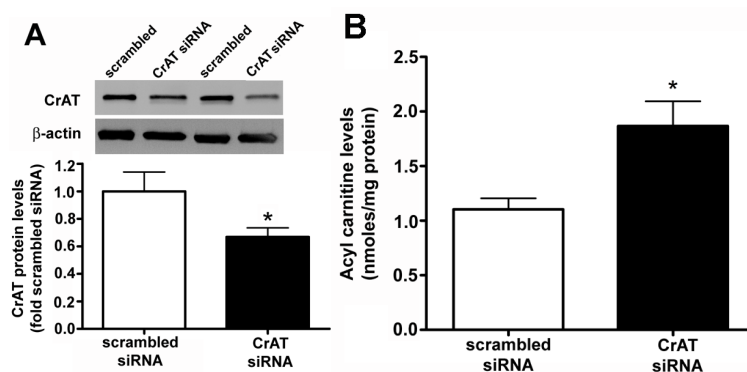
Previously, we have developed a clinically relevant animal model of a CHD with increased PBF, by placing a large aorto-pulmonary vascular graft (shunt) in the late-gestation fetal lamb [14], which allows the study of early mechanisms of pulmonary vascular disease. In this model, we have shown a selective impairment of endothelium-mediated pulmonary vasodilation [15,16], associated with decreased NO signaling and increased oxidative stress [2,17,18]. We have recently found mitochondrial dysfunction in these shunt lambs which was associated with the disruption of carnitine homeostasis [19]. We also correlated the disruption of carnitine homeostasis with significant decreases in both CrAT expression and activity as well as reduced NO signaling [19]. Thus, the objective of this study was to determine if loss of CrAT enzyme activity was sufficient to disrupt carnitine homeostasis, mitochondrial function, and NO signaling using a siRNA-based approach in cultured pulmonary arterial endothelial cells (PAEC).

2. Results

2.1. CrAT siRNA Significantly Decreases CrAT Protein Levels and Disrupts Carnitine Homeostasis in Pulmonary Arterial Endothelial Cells

PAEC were transiently transfected with a scrambled or CrAT siRNA and the level of CrAT knockdown was determined by measuring protein levels. There was a significant reduction in CrAT protein in CrAT siRNA transfected cells (Figure 1A). Carnitine is present in the form of either free carnitine or acylcarnitines. Enzymatic alterations in carnitine metabolism can result in higher levels of acylated carnitines and it is important that the potentially toxic acyl-groups are removed from the system by the administration of carnitine. To determine if the knockdown of CrAT gene resulted in disruption of cellular carnitine homeostasis, we determined acylcarnitine levels using HPLC analysis. Our data indicate that CrAT siRNA transfection led to a significant increase in acylcarnitine levels (Figure 1B), thus confirming that decreasing CrAT activity is sufficient to disrupt carnitine homeostasis in PAEC.

Figure 1. Carnitine acetyl transferase (CrAT) gene silencing decreases CrAT protein levels and disrupts carnitine homeostasis in pulmonary arterial endothelial cells. PAEC were transfected with a scrambled small interfering RNA (siRNA) or a specific CrAT siRNA for 48 h and the level of CrAT knockdown was confirmed by measuring CrAT protein levels. There was a significant reduction in CrAT protein (A) β -actin as used to normalize protein loading. The decrease in CrAT protein correlated with a disrupted carnitine homeostasis as demonstrated by an increase in the cellular levels of acylcarnitines (B) Values are mean \pm SEM; $N = 6-11$. * $p < 0.05$ vs. scrambled siRNA.



2.2. CrAT Knockdown Disrupts Superoxide Dismutase Function and Increases Mitochondrial Oxidative Stress in Pulmonary Arterial Endothelial Cells

SOD2 is known to be a major mitochondrial superoxide scavenger enzyme that protects the cells against oxidative stress. We found that suppressing CrAT activity led to a significant decrease in SOD2 mRNA (Figure 2A), SOD2 protein (Figure 2B) and SOD2 activity (Figure 2C). In turn we were able to show the decrease in SOD2 activity led to a significant increase in mitochondrial superoxide levels (Figure 2D) indicating that CrAT-regulated loss of SOD2 resulted in increased oxidative stress within the mitochondria. Further, our data indicate that CrAT gene silencing produces significant decrease both in O_2 consumed for ATP production (Figure 3A) and cellular ATP levels (Figure 3B). Together these

data indicate that the loss of carnitine homeostasis induced by suppressing CrAT activity, leads to the disruption of mitochondrial function.

Figure 2. Decreased CrAT activity attenuates SOD2 expression and activity in pulmonary arterial endothelial cells. PAEC were transiently transfected with a scrambled siRNA or a specific CrAT siRNA for 48 h. Decreasing CrAT expression resulted in significant decreases in (A) SOD2 mRNA; (B) protein and (C) SOD2 activity. The decrease in SOD2 activity also significantly increased mitochondrial superoxide levels (D) as determined using the MitoSOX red mitochondrial superoxide indicator. Values are mean ± SEM; N = 6–12. * $p < 0.05$ vs. scrambled siRNA.

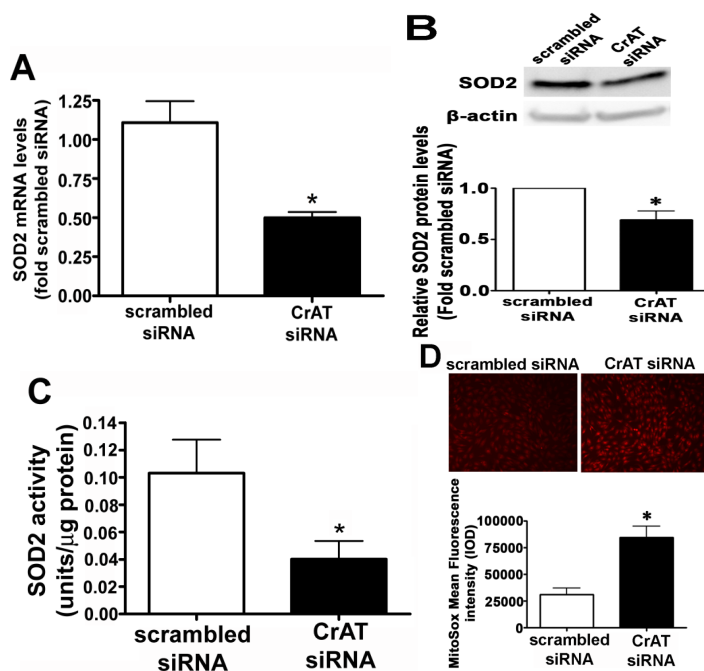
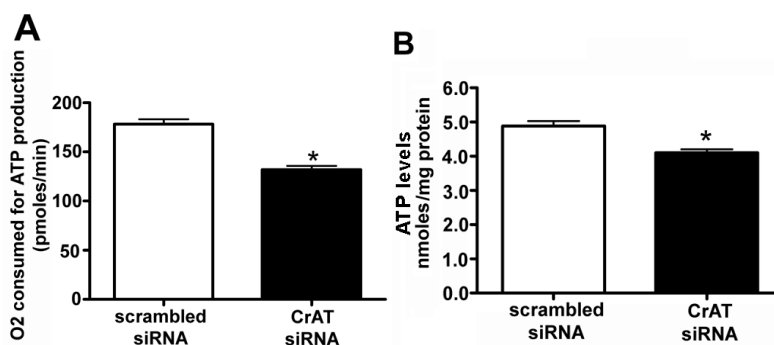


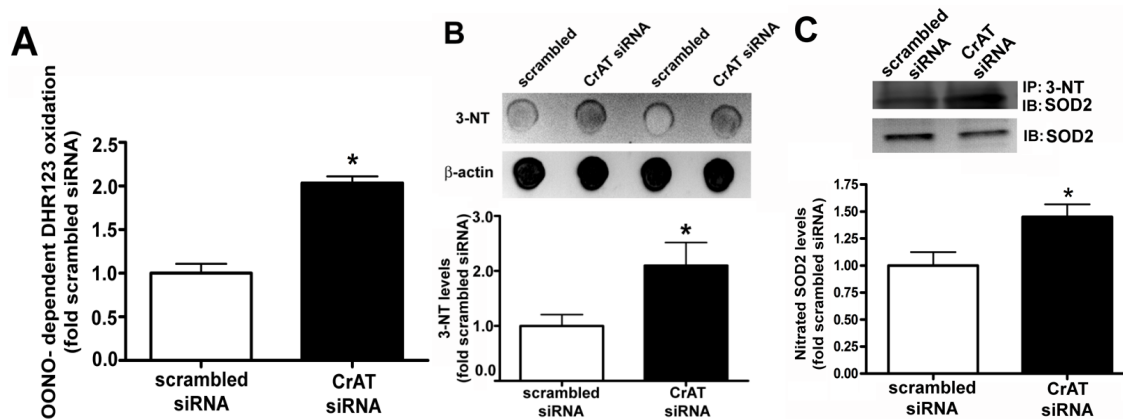
Figure 3. Decreased CrAT activity disrupts mitochondrial bioenergetics and ATP generation in pulmonary arterial endothelial cells. PAEC were transiently transfected with a scrambled siRNA or a specific CrAT siRNA for 48 h and the effect on mitochondrial respiration determined using the Seahorse XF24 analyzer. In the CrAT siRNA transfected cells there was a significant decrease in the (A) amount of oxygen consumed (OCR) for ATP production and (B) this corresponded with a reduction in cellular ATP levels. Values are mean ± SEM; N = 6. * $p < 0.05$ vs. scrambled siRNA.



2.3. Suppressing CrAT Expression Causes Nitritative Stress in Pulmonary Arterial Endothelial Cells

To determine if the increase in oxidative stress associated with mitochondrial dysfunction also resulted in increased nitritative stress, we next determined cellular peroxynitrite levels using the oxidation of DHR 123 to rhodamine 123 and protein nitration using an antibody specific for 3-NT residues. Our data indicate that silencing the CrAT gene increased both peroxynitrite (Figure 4A) and total protein nitration (Figure 4B). Further, despite less SOD2 present in CrAT siRNA transfected cells (Figure 2A,B), the increase in cellular peroxynitrite generation increased SOD2 nitration (Figure 4C).

Figure 4. CrAT gene silencing causes nitritative stress in pulmonary arterial endothelial cells. PAEC were transiently transfected with a scrambled siRNA or a specific CrAT siRNA for 48 h and the effect on cellular peroxynitrite levels determined. There was an increase in peroxynitrite generation (A) as determined by DHR123 oxidation and a corresponding increase in total nitrated proteins; (B) as determined by Dot Blot analysis (C) This increase in peroxynitrite generation resulted in a significant increase of SOD2 nitration. Values are mean \pm SEM; $N = 6-11$. * $p < 0.05$ vs. scrambled siRNA.



2.4. CrAT Mediated Mitochondrial Dysfunction Disrupts eNOS/Hsp90 Interactions and Leads to eNOS Uncoupling

Hsp90 is an ATP dependent chaperone and the interaction of Hsp90 with eNOS has been shown to increase eNOS coupling and NO production [20]. Thus, we next examined the effect of the decrease in cellular ATP levels on eNOS/Hsp90 interactions. CrAT gene silencing did not alter total eNOS (Figure 5A) or Hsp90 (Figure 5B) protein levels in PAEC. However, immunoprecipitation analyses revealed that siRNA mediated CrAT knockdown significantly decreased the interaction of Hsp90 to eNOS (Figure 5C). Further, we found that this disruption in eNOS/Hsp90 interaction induced a significant increase in NOS-derived superoxide levels (Figure 6A) and a significant reduction in NO generation (Figure 6B) when PAEC were acutely exposed to fluid shear stress. Together these data indicate that the impaired mitochondrial function induced by decreased CrAT activity leads to uncoupling of eNOS and reduced NO signaling.

Figure 5. CrAT gene knockdown disrupts eNOS/Hsp90 interactions in pulmonary arterial endothelial cells. PAEC were transiently transfected with a scrambled siRNA or a specific CrAT siRNA for 48 h. Western blot analysis revealed that reducing CrAT expression did not alter total protein levels of (A) eNOS or (B) Hsp90 (C) However, immunoprecipitation (IP) analysis using a specific antiserum raised against Hsp90 followed by Western blot (IB) analysis with an anti-eNOS antibody revealed that there was a significant decrease in the association of eNOS with Hsp90 in CrAT siRNA transfected cells. The membrane was then reprobbed for Hsp90 to normalize for immunoprecipitation efficiency. Values are mean ± SEM; N = 6. * p < 0.05 vs. scrambled siRNA.

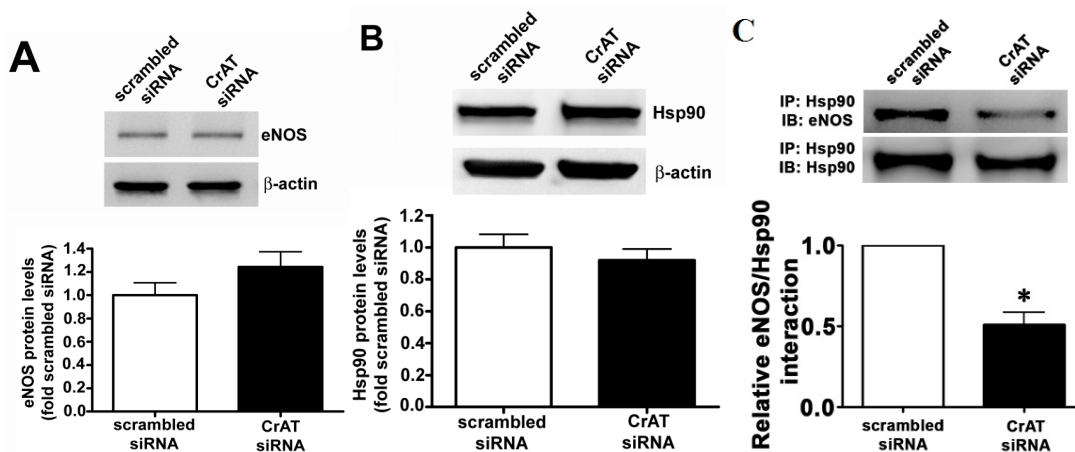
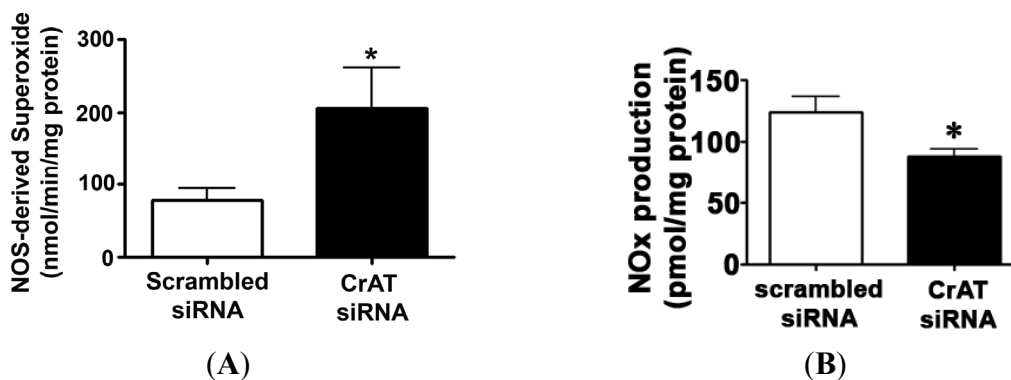


Figure 6. CrAT gene silencing attenuates shear stress induced NO signaling in pulmonary arterial endothelial cells. PAEC were transiently transfected with a scrambled siRNA or a specific CrAT siRNA for 48 h then acutely exposed to laminar shear stress (20 dyn/cm², 15 min) in the presence or absence of the NOS inhibitor 2-ethyl-2-thiopseudourea (ETU; 100 μM, 30 min) and the effect on eNOS-derived superoxide generation determined by EPR (A) Decreasing CrAT activity significantly increased superoxide levels. The presence of ETU significantly inhibited the increase in superoxide levels in the CrAT siRNA transfected cells, indicating that it is eNOS-dependent (B) Conversely, the shear-mediated increase in NO_x was significantly decreased in CrAT siRNA transfected PAEC. Values are mean ± SEM; N = 6; * p < 0.05 vs. scrambled siRNA.



3. Discussion

Carnitine plays a vital role in cellular energy production. In the mitochondria, carnitine exists in a balance with acetyl-L-carnitine and acetyl-CoA that is involved in regulating mitochondrial activity and fat burning. Studies have shown that carnitine has a protective effect both on mitochondria and in whole cells by inhibiting free fatty acid induced mitochondrial membrane damage and/or its secondary effects [21–23]. Recent experimental and clinical studies have shown that mitochondrial dysfunction secondary to a disruption of carnitine homeostasis may play a role in decreased NO signaling and the development of endothelial dysfunction [19,24]. Carnitine is present in the organism as free carnitine (FC) or as acylcarnitines (AC, esterified form), which along with carnitine-dependent enzymes and plasma membrane transporters constitute the carnitine system. Adequate carnitine levels, as well as optimal activities of carnitine-dependent enzymes are required to maintain balanced carnitine homeostasis. The main function of L-carnitine is the transport of long-chain fatty acids from the cytosol to the mitochondrial matrix for β -oxidation and ATP production. L-carnitine however, also plays a key regulatory role in intermediary metabolism by modulating cellular acyl-CoA/CoA ratio. This function is mostly dependent on the freely reversible conversion of short-chain acyl-CoA and carnitine to free CoA and acylcarnitine by the intra-mitochondrial enzyme, CrAT. The acetyl-carnitine shuttle in which acetyl-CoA is reversibly converted to acetyl-carnitine by carnitine acetyl transferase (CrAT) enzymes is important for intracellular transport of acetyl units.

Coenzyme A is an obligate cofactor for many enzymes involved in intermediary metabolism. It remains compartmentalized in limited pools within the cell, mainly in the mitochondria, and is normally kept in homeostasis with carnitine. The reversible transfer of acyl groups from CoA to carnitine ensures the vital maintenance of free CoA pools within the mitochondria and prevents the accumulation of poorly metabolized short-chain acyl-CoA compounds, which are exported out of the mitochondria as carnitine esters. Therefore, the carnitine system is crucial for normal mitochondrial function, as the accumulation of acyl groups and the unavailability of free CoA result in a metabolic roadblock within the mitochondria, with subsequent impaired oxidative metabolism, increased mitochondrial ROS generation, and decreased energy production [25–27]. We recently identified a disruption in carnitine homeostasis in shunt lambs that correlated with mitochondrial dysfunction, oxidative stress, and impaired NO signaling [19]. These lambs showed high acylcarnitine: free carnitine ratio, reflecting an imbalance in mitochondrial acylCoA/CoA, as well as decreased carnitine-dependent enzymes (CPT1, CPT2 and CrAT) and a significant decrease in CrAT activity [19]. Despite compelling evidence that oxidative stress plays a causal role in the development of pulmonary vascular disease secondary to increased PBF [2], this study was the first to suggest a mitochondrial component linked to alterations in the carnitine system in its pathogenesis. Previously, lung mitochondrial dysfunction had only been reported in the pulmonary hypertension syndrome of fast-growing broilers syndrome, which was interestingly attenuated by antioxidant therapy with vitamin E [28]. Different mechanisms could explain the disrupted carnitine homeostasis in our lamb model of increased PBF as we have observed changes in CPT1, CPT2, and CrAT. However, the cell culture data presented here suggest decreasing CrAT activity is sufficient to induce mitochondrial dysfunction and NO signaling.

In the present study, we found that knockdown of CrAT using siRNA approach resulted in an increase in peroxynitrite and total nitrated proteins thus, suggesting higher nitrative stress in the

endothelial cells. SODs play a critical role in inhibiting oxidative inactivation of NO, thereby preventing peroxynitrite formation. Both oxidative and nitrative stress within the mitochondria can cause mitochondrial dysfunction by damaging mitochondrial proteins and thereby altering electrochemical gradient. A study undertaken to examine the oxidation-induced apoptosis in cultured mouse retinal pigment epithelial cells, has shown that the deficiency of SOD2 resulted in greater disruption of the membrane potential, whereas over-expression of the enzyme protected against mitochondrial membrane damage. It was also reported that the extent of the mitochondrial damage was related to the level of SOD2 [29]. We found that CrAT gene silencing decreased SOD2 expression and increased SOD2 nitration. Together these changes produce a decrease in SOD2 activity. This link between carnitine homeostasis, SOD2, and mitochondrial dysfunction may play an important role in the development of pulmonary hypertension as we have shown early derangements in SOD2 in our lamb model of pulmonary hypertension [30] while a recent study found that SOD2 expression and activity was decreased in PAEC isolated from patients with idiopathic pulmonary arterial hypertension (IPAH) [31]. Similarly, both carnitine metabolism and fatty acid oxidation are significantly depressed in human pulmonary vascular endothelial cells containing a bone morphogenetic protein receptor type 2 (BMP2) mutation [32] again suggesting a link between carnitine metabolism and mitochondrial dysfunction in pulmonary hypertension.

It has been previously shown that SOD2, which plays a critical role in cellular defense against oxidative stress by decomposing superoxide within mitochondria, is nitrated and inactivated under pathological conditions [33]. Therefore, our data suggest that CrAT might be regulating SOD2 both at transcriptional (protein) and post-translational (nitration) levels. Indeed, several previously published studies support this finding. For example, L-carnitine has been shown to enhance SOD activity in a number of cell types [34–36] suggesting that there is a link between carnitine homeostasis and the regulation of SOD gene expression. Similar to our results, a previous study has also shown that a reduction in SOD2 levels results in increased superoxide and peroxynitrite concentrations and decreased NO concentration in the vessel wall [37]. It has also been reported that the manganese ion in SOD2 enzyme plays an important role in the decomposition kinetics of peroxynitrite and in peroxynitrite-dependent nitration of self and remote tyrosine residues [38].

In this study we also found a significant decrease in ATP levels in CrAT siRNA transfected cells which corresponded to a reduction in oxygen consumption rate (OCR) related to ATP synthase. Previous studies have shown the importance of ATP in pulmonary endothelial function, at least in part, through its ability to stimulate NO release via the activation of eNOS [39]. Endothelial NOS activity is tightly controlled through multiple mechanisms that include phosphorylation and protein-protein interactions [40]. Hsp90, a member of a molecular chaperone family, is among the proteins that increase eNOS activity by facilitating the displacement of caveolin-1 from eNOS, in a process that is ATP dependent [41]. Therefore, it is plausible that the reduction in ATP levels associated with reduced CrAT expression decreases Hsp90/eNOS interactions and attenuates NO production [19]. Further, it is suggestive that L-carnitine supplementation could improve endothelial function. A number of studies have evaluated L-carnitine as a therapeutic tool in conditions characterized by mitochondrial dysfunction and oxidative stress. In addition to reducing the toxicity resulting from excess acyl-CoA, exogenous L-carnitine has been shown to have antioxidant and anti-apoptotic properties [11,42,43]. The mechanisms by which L-carnitine protect cells against ROS is not completely clear, but may include direct free radical

scavenging and inhibition and/or repair of peroxidized biomolecules [43,44]. Exogenous L-carnitine has shown a beneficial effect in both animal and human studies in conditions as diverse as Alzheimer disease, hypoxic-ischemic brain injury, diabetes, aging, chronic renal failure, atherosclerosis or ischemic heart disease [21,43–50]. In each case oxidative stress was reduced and mitochondrial performance was enhanced. L-carnitine supplementation in systemic hypertensive rats has also been previously shown to enhance NO production, while attenuating oxidative stress and endothelial dysfunction [51,52].

4. Methods

4.1. Culture of Pulmonary Arterial Endothelial Cells

Primary cultures of ovine pulmonary arterial endothelial cells (PAEC) were isolated as described previously [53]. All cultures were maintained in DMEM supplemented with 10% fetal calf serum (Hyclone, Logan, UT, USA) antibiotics/antimycotic (500 IU Penicillin, 500 µg/mL Streptomycin, 1.25 µg/mL Amphotericin B; MediaTech, Herndon, VA, USA) at 37 °C in a humidified atmosphere with 5% CO₂ and 95% air. Cells between passages 3 and 10 were used for all experiments.

4.2. Targeted Silencing of Carnitine Acetyl Transferase by Small-Interfering RNA

PAEC were grown in 6-well plates to ~60% confluence and transfected with optimized concentrations of a custom made small interfering RNA (siRNA) specific for ovine CrAT (s100014889, Santa Cruz Biotechnology, Santa Cruz, CA, USA) or as a control, a scrambled siRNA (sc-37007, Santa Cruz Biotechnology, Santa Cruz, CA, USA) with no known homology to any sequences from mouse, rat, or human RNA. Transfections were performed using the HiPerfect transfection reagent (cat # 301705, Qiagen, Valencia, CA, USA) and 25 nM of the appropriate siRNA. Whole cell lysates were prepared after 48 h of transfection, and CrAT knockdown confirmed using Western blot analysis.

4.3. Sample Purification and Measurement of Carnitine Metabolites

For free carnitine determination, 100 µL cell lysates, 300 µL of water, and 100 µL of an internal standard (Sigma ST 1093) were mixed. For total carnitine determinations, 100 µL cell lysates were hydrolyzed with 0.3 M KOH, heated at 45 °C, and pH neutralized using 0.8 M perchloric acid; the final volume was made to 400 µL and 100 µL of an internal standard was added. The total volume of each reaction mixture should be 500 µL. All samples were purified using solid-phase extraction columns (SAX, 100 mg/mL; Varian, Harbor City, CA, USA), derivatized using aminoanthracene in the presence of a catalyst; 1-[3-(dimethylamino)propyl]-3-ethylcarbodiimide hydrochloride (EDCI), and kept at 30 °C for an hour. Separation was carried out using an isocratic elution in 0.1 M Tris-acetate buffer (pH 3.5): acetonitrile (68:32, v/v) at a flow rate of 0.9 mL/min as described previously [19]. Detection of carnitines was performed using a Shimadzu UFLC system with a 5 µm Omnispher C18 column (250 × 4.6 mm OD) and equipped with an RF-10AXL fluorescence detector (Shimadzu USA Manufacturing Corporation, Canby, OR, USA). Total and free carnitine levels were quantified by fluorescence detection at 248 nm (excitation) and 418 nm (emission). The acylcarnitines were calculated by subtracting the free carnitine values from the total carnitine values for all the samples.

4.4. Measurement of Peroxynitrite Levels

The formation of peroxynitrite was determined by the oxidation of dihydrorhodamine (DHR) 123 to rhodamine 123, as described previously [54]. Cultured PAEC were transfected with either scrambled or CrAT siRNA for 48 h. The cells were then treated with PEG-Catalase (100 U, 30 min) to reduce H₂O₂ dependent DHR 123 oxidation. Five micromole per litre DHR 123 was added to the cells in phenol red-free media and the fluorescence of rhodamine 123 was measured at excitation 485 nm and emission 545 nm after 30 min of incubation using a Fluoroskan Ascent Microplate Fluorometer. The fluorescent values were normalized to the protein levels in the samples.

4.5. Measurement of 3-NT Levels

The total nitrated protein levels were measured in the PAEC transfected with either scrambled or CrAT siRNA via a dot blot procedure. Briefly, 50 µg protein lysate was applied to a nitrocellulose membrane pre-soaked with Tris-buffered saline (TBS). After the protein samples were completely transferred, the membrane was blocked in 5% fat-free milk for 1 h, washed with TBS, and incubated with mouse anti-3-nitrotyrosine (1:100, Calbiochem) antibody overnight. Finally, the membrane was incubated with goat anti-mouse IgG for 2 h. The reactive dots were visualized using chemiluminescence (Pierce Laboratories, Rockford, IL, USA) on a Kodak 440 CF image station (New Haven, CT, USA). The band intensity was quantified using Kodak 1D image processing software. Protein loading was normalized by re-probing with mouse anti β-actin antibody.

4.6. Real Time Quantitative (q) RT-PCR for mRNA Levels

Quantitative RT-PCR using SYBR green I dye for specific detection of double-stranded DNA was employed to determine SOD2 mRNA levels in scrambled siRNA and CrAT siRNA transfected (48 h) PAEC. Briefly, total RNA was extracted using the RNeasy kit (Qiagen), and 1 µg total RNA was reverse-transcribed using QuantiTect Reverse Transcription Kit (Qiagen) in a total volume of 20 µL. Primers for SOD2 and β-actin were designed by IDT (Coralville, IA, USA). The sequences were SOD2 Forward, 5'-GTTGGCTCGGCTTCAATAAG-3', Reverse, 5'-AATCGGGCCTGACATTTTAA-3'; β-actin Forward, 5'-GGGAAATCGTGCGTGACATTAAG-3', Reverse, 5'-TGTGTTGGCGTAAGGT CTTTG-3'. Real-time PCR and melting curve analyses were carried out using an Mx4000 Multiplex Quantitative PCR System (Stratagene), using 2 µL of RT product, 12.5 µL of QuantiTect SYBR Green PCR Master Mix (Qiagen) and primers (400 nM) in a total volume of 25 µL. The following thermocycling conditions were employed: 95 °C for 10 min, followed by 95 °C for 30 s, 55 °C for 60 s and 72 °C 30 s for 40 cycles. There were 2^{-ΔΔCT} values chosen to reflect the number of mRNA molecules using β-actin (housekeeping gene) as an internal control.

4.7. Western Blot Analyses

Protein extracts were prepared by homogenizing CrAT siRNA transfected PAEC in Triton lysis buffer (50 mM Tris-HCL, pH 7.6, 0.5% Triton-X100, 20% glycerol) containing a protease inhibitor cocktail. Extracts were then clarified by centrifugation (15,000 rpm for 10 min at 4 °C). Supernatant fractions were then assayed for protein concentration using the Pierce BCA protein assay kit

(ThermoScientific, Rockford, IL, USA), and Western blot analysis was performed as previously described [55–57]. Briefly, protein extracts (25–50 µg) were separated on Long-Life 4%–20% Tris-SDS-Hepes gels (Frenchs Forest, Australia). All gels were electrophoretically transferred to Immuno-Blot™ PVDF membrane (Bio-Rad Laboratories, Hercules, CA, USA). The membranes were blocked with 5% nonfat dry milk in Tris-buffered saline containing 0.1% Tween 20 (TBST). After blocking, the membranes were probed at room temperature with antibodies to CrAT (Proteintech, Chicago IL, USA); SOD2 (Upstate, Lake Placid, NY, USA); eNOS or Hsp90 (BD Transduction, San Jose, CA, USA); washed with TBS containing 0.1% Tween, and then incubated with an appropriate IgG conjugated to horseradish peroxidase. Protein bands were then visualized with chemiluminescence (SuperSignal® West Femto Substrate Kit, Pierce Laboratories, Rockford, IL, USA) on a Kodak 440 CF Image Station (Kodak, Rochester, NY, USA). Band intensity was quantified using Kodak 1D image processing software. All captured and analyzed images were determined to be in the dynamic range of the system. To normalize for protein loading, blots were re-probed with the housekeeping protein, β-actin.

4.8. Measurement of SOD2 Activity

SOD2 activity was measured in whole cell homogenates from scrambled and CrAT siRNA transfected PAEC using a SOD activity kit (Enzo Life Sciences, Farmingdale, NY, USA) according to the manufacturer's instructions. Absorbance was read at 450 nm and SOD2 activity presented as units per microgramme protein.

4.9. Immunoprecipitation Analysis

To determine the levels of nitrated SOD2 and eNOS/Hsp90 interactions after CrAT siRNA transfections, PAEC were homogenized in immunoprecipitation buffer 25 mM HEPES, pH 7.5, 150 mM NaCl, 1% Nonidet P-40, 10 mM MgCl₂, 1 mM EDTA, and 2% glycerol supplemented with protease inhibitor cocktail (Pierce Laboratories, Rockford, IL, USA). Cell homogenates (500 µg of protein) were precipitated with either 3-nitrotyrosine or rabbit antibody against Hsp90 in 0.5 mL final volume at 4 °C overnight. Protein G plus/protein A agarose (40 µL; Calbiochem) was added and rotated at 4 °C for an additional 2 h. The precipitated protein was washed three times in 2× volume of immunoprecipitation buffer; the pellet was re-suspended in Laemmli buffer (20 µL), boiled, and separated on a 4%–20% SDS-PAGE gel (LongLife). eNOS protein levels were then detected using Western blot analysis as described above. The efficiency of immunoprecipitation was normalized by re-probing the membranes with anti-Hsp90 antibody. The nitrated SOD2 blot was normalized by running the same samples in a separate gel for total SOD2 protein levels.

4.10. Determination of Mitochondrial Superoxide

MitoSOX™ Red mitochondrial superoxide indicator (Molecular Probes), a fluorogenic dye for selective detection of superoxide in the mitochondria of live cells was used. The MitoSOX Red reagent is live-cell permeant and is rapidly and selectively targeted to the mitochondria. Once in the mitochondria, MitoSOX Red reagent is oxidized by superoxide and exhibits bright red fluorescence upon binding to nucleic acids. After siRNA mediated CrAT silencing, cells were washed with fresh

media, and then incubated in media containing MitoSOX Red (5 μ M), for 30 min at 37 °C in dark conditions. Cells were washed with fresh serum-free media and imaged using fluorescence microscopy at an excitation of 510 nm and an emission at 580 nm. A PC-based imaging system consisting of the following components was used for the fluorescent analyses: an Olympus IX51 microscope equipped with a CCD camera (Hamamatsu Photonics, Bridgewater, NJ, USA) was used for acquisition of fluorescent images. The average fluorescent intensities (to correct for differences in cell number) were quantified using ImagePro Plus version 5.0 imaging software (Media Cybernetics, Rockville, MD, USA) as previously published [58].

4.11. Mitochondrial Bioenergetic Analysis in Transfected Cells

The XF24 Analyzer (Seahorse Biosciences, North Billerica, MA, USA) was used to measure bioenergetics function in scrambled and CrAT siRNA transfected endothelial cells. In preliminary studies, the optimum number of cells/well was determined as 75,000/0.32 cm². This cell number allows the appropriate detection of changes in oxygen consumption rate (OCR). Then the electron transport chain uncouplers and inhibitors such as Oligomycin, FCCP (carbonyl cyanide 4-(trifluoromethoxy phenylhydrazine) and rotenone + antimycin A were injected sequentially through ports of the Seahorse Flux Pak cartridges to reach final concentrations of 1 μ M each. Using these agents, we determined the amount of oxygen consumption linked to ATP production and the data presented as picomoles per minute.

4.12. Determination of Cellular ATP Levels

ATP levels were estimated using the firefly luciferin-luciferase method utilizing a commercially available kit (Invitrogen) as previously published [19]. ATP is consumed and light is emitted when firefly luciferase catalyzes the oxidation of luciferin. The amount of light emitted during the reaction is proportional to the availability of ATP. Luminescence was determined using a Fluoroscan Ascent FL plate luminometer (ThermoFisher Scientific, Waltham, MA, USA). ATP levels were presented as nanomoles per milligram of protein.

4.13. Shear Stress

PAEC were exposed to laminar shear stress using a cone-plate viscometer that accepts six-well tissue culture plates, as described previously [59]. This method achieves laminar flow rates that represent physiological levels of laminar shear stress in the major human arteries, which is in the range of 5–20 dyn/cm² [60]. Cells were acutely exposed to shear stress (20 dyn/cm², 15 min) and both NOS-derived superoxide and NO_x levels determined.

4.14. Measurement of NOS-Derived Superoxide Levels in PAEC

This was estimated by electron paramagnetic resonance (EPR) assay using the spin-trap compound 1-hydroxy-3-methoxycarbonyl-2,2,5,5-tetramethylpyrrolidine HCl (CMH, Enzo Life Sciences, Inc., Farmingdale, NY, USA) as described previously [20,61]. Superoxide produced in PAEC was trapped by incubating cells with 20 μ L of CMH stock solution (20 mg/mL) for 1 h. The cells were then trypsinized

and centrifuged at 500g for 5 min. The cell pellet was suspended in 35 μ L DPBS and loaded into a capillary tube which was then analyzed with a MiniScope MS200 EPR machine (Magnetech, Berlin, Germany). NOS-derived superoxide was measured by pre-incubating lysate with 100 μ M ethylisothiourea (ETU, Sigma-Aldrich, St. Louis, MO, USA) for 30 min followed by incubation with CMH. EPR spectra were analyzed using ANALYSIS v.2.02 software (Magnetech: Berlin, Germany, 2005). Differences between levels of samples incubated in the presence and absence of ETU were used to determine NOS-dependent superoxide generation. Superoxide levels were reported as nmols superoxide/min/mg protein.

4.15. Determination of Cellular NO_x Levels

NO and its metabolites were determined in PAEC homogenates to quantify bioavailable NO. In solution, NO reacts with molecular oxygen to form nitrite, and with oxyhaemoglobin and superoxide anion to form nitrate. Nitrite and nitrate are reduced using vanadium (III) and hydrochloric acid at 90 °C. NO is purged from solution resulting in a peak of NO for subsequent detection by chemiluminescence (NOA 280, Sievers Instruments Inc., Boulder, CO, USA), as we have previously described [62,63]. The sensitivity is 1×10^{-12} moles, with a concentration range of 1×10^{-9} to 1×10^{-3} molar of nitrate.

4.16. Statistical Analysis

Statistical analysis was performed using GraphPad Prism version 4.01 for Windows (GraphPad Software: San Diego, CA, USA). The mean \pm SEM was calculated for all samples and significance was determined by the unpaired *t*-test. A value of $p < 0.05$ was considered significant.

5. Conclusion

Our results indicate that CrAT is an important enzyme that is not only involved in optimizing mitochondrial function, but is also involved in maintaining SOD2 expression and decreasing mitochondrial oxidative stress. Further, by maintaining cellular ATP levels, both Hsp90 activity and NO signaling are preserved. We suggest that chronic L-carnitine therapy may improve and/or attenuate the decline in endothelial function noted in children with CHD and increased PBF, and thus may have important clinical implications that warrant further investigation.

Acknowledgments

This research was supported in part by grants, HL60190 (to SMB), HL67841 (to SMB), HL084739 (to SMB), R21HD057406 (to SMB) and HL61284 (to JRF) all from the National Institutes of Health, by a grant from the Fondation Leducq (to SMB), an AHA Scientist Development Grant 11SDG7460024 (to SS), and GHSU Cardiovascular Discovery Institute Seed Awards (to SS and SK).

Conflict of Interest

The authors declare no conflict of interest.

References

1. Hanley, F.L.; Heinemann, M.K.; Jonas, R.A.; Mayer, J.E., Jr.; Cook, N.R.; Wessel, D.L.; Castaneda, A.R. Repair of truncus arteriosus in the neonate. *J. Thorac. Cardiovasc. Surg.* **1993**, *105*, 1047–1056.
2. Black, S.M.; Fineman, J.R. Oxidative and nitrosative stress in pediatric pulmonary hypertension: Roles of endothelin-1 and nitric oxide. *Vasc. Pharmacol.* **2006**, *45*, 308–316.
3. Celermajer, D.S.; Cullen, S.; Deanfield, J.E. Impairment of endothelium-dependent pulmonary artery relaxation in children with congenital heart disease and abnormal pulmonary hemodynamics. *Circulation* **1993**, *87*, 440–446.
4. Lakshminrusimha, S.; Wiseman, D.; Black, S.M.; Russell, J.A.; Gugino, S.F.; Oishi, P.; Steinhorn, R.H.; Fineman, J.R. The role of nitric oxide synthase-derived reactive oxygen species in the altered relaxation of pulmonary arteries from lambs with increased pulmonary blood flow. *Am. J. Physiol. Heart Circ. Physiol.* **2007**, *293*, H1491–H1497.
5. Zhang, D.X.; Gutterman, D.D. Mitochondrial reactive oxygen species-mediated signaling in endothelial cells. *Am. J. Physiol. Heart Circ. Physiol.* **2007**, *292*, H2023–H2031.
6. Puddu, P.; Puddu, G.M.; Cravero, E.; de Pascalis, S.; Muscari, A. The putative role of mitochondrial dysfunction in hypertension. *Clin. Exp. Hypertens.* **2007**, *29*, 427–434.
7. Genova, M.L.; Pich, M.M.; Bernacchia, A.; Bianchi, C.; Biondi, A.; Bovina, C.; Falasca, A.I.; Formiggini, G.; Castelli, G.P.; Lenaz, G. The mitochondrial production of reactive oxygen species in relation to aging and pathology. *Ann. N. Y. Acad. Sci.* **2004**, *1011*, 86–100.
8. Mancuso, C.; Scapagini, G.; Curro, D.; Giuffrida Stella, A.M.; de Marco, C.; Butterfield, D.A.; Calabrese, V. Mitochondrial dysfunction, free radical generation and cellular stress response in neurodegenerative disorders. *Front. Biosci.* **2007**, *12*, 1107–1123.
9. Puddu, P.; Puddu, G.M.; Cravero, E.; de Pascalis, S.; Muscari, A. The emerging role of cardiovascular risk factor-induced mitochondrial dysfunction in atherogenesis. *J. Biomed. Sci.* **2009**, *16*, 112.
10. Sims, N.R.; Muyderman, H. Mitochondria, oxidative metabolism and cell death in stroke. *Biochim. Biophys. Acta* **2010**, *1802*, 80–91.
11. Calo, L.A.; Pagnin, E.; Davis, P.A.; Semplicini, A.; Nicolai, R.; Calvani, M.; Pessina, A.C. Antioxidant effect of L-carnitine and its short chain esters: Relevance for the protection from oxidative stress related cardiovascular damage. *Int. J. Cardiol.* **2006**, *107*, 54–60.
12. Rodriguez-Iturbe, B.; Zhan, C.D.; Quiroz, Y.; Sindhu, R.K.; Vaziri, N.D. Antioxidant-rich diet relieves hypertension and reduces renal immune infiltration in spontaneously hypertensive rats. *Hypertension* **2003**, *41*, 341–346.
13. Alvarez de Sotomayor, M.; Bueno, R.; Perez-Guerrero, C.; Herrera, M.D. Effect of L-carnitine and propionyl-L-carnitine on endothelial function of small mesenteric arteries from SHR. *J. Vasc. Res.* **2007**, *44*, 354–364.
14. Reddy, V.M.; Meyrick, B.; Wong, J.; Khor, A.; Liddicoat, J.R.; Hanley, F.L.; Fineman, J.R. In utero placement of aortopulmonary shunts. A model of postnatal pulmonary hypertension with increased pulmonary blood flow in lambs. *Circulation* **1995**, *92*, 606–613.

15. Black, S.; Fineman, J.; Johengen, M.; Bristow, J.; Soifer, S. Increased pulmonary blood flow alters the molecular regulation of vascular reactivity in the lamb. *Chest* **1998**, *114*, 39S.
16. Reddy, V.M.; Wong, J.; Liddicoat, J.R.; Johengen, M.; Chang, R.; Fineman, J.R. Altered endothelium-dependent responses in lambs with pulmonary hypertension and increased pulmonary blood flow. *Am. J. Physiol.* **1996**, *271*, H562–H570.
17. Grobe, A.C.; Wells, S.M.; Benavidez, E.; Oishi, P.; Azakie, A.; Fineman, J.R.; Black, S.M. Increased oxidative stress in lambs with increased pulmonary blood flow and pulmonary hypertension: Role of NADPH oxidase and endothelial NO synthase. *Am. J. Physiol. Lung Cell. Mol. Physiol.* **2006**, *290*, L1069–L1077.
18. Oishi, P.E.; Wiseman, D.A.; Sharma, S.; Kumar, S.; Hou, Y.; Datar, S.A.; Azakie, A.; Johengen, M.J.; Harmon, C.; Fratz, S.; *et al.* Progressive dysfunction of nitric oxide synthase in a lamb model of chronically increased pulmonary blood flow: A role for oxidative stress. *Am. J. Physiol. Lung Cell. Mol. Physiol.* **2008**, *295*, L756–L766.
19. Sharma, S.; Sud, N.; Wiseman, D.A.; Carter, A.L.; Kumar, S.; Hou, Y.; Rau, T.; Wilham, J.; Harmon, C.; Oishi, P.; *et al.* Altered carnitine homeostasis is associated with decreased mitochondrial function and altered nitric oxide signaling in lambs with pulmonary hypertension. *Am. J. Physiol. Lung Cell. Mol. Physiol.* **2008**, *294*, L46–L56.
20. Sud, N.; Sharma, S.; Wiseman, D.A.; Harmon, C.; Kumar, S.; Venema, R.C.; Fineman, J.R.; Black, S.M. Nitric oxide and superoxide generation from endothelial NOS: Modulation by HSP90. *Am. J. Physiol. Lung Cell. Mol. Physiol.* **2007**, *293*, L1444–L1453.
21. Binienda, Z.; Przybyla-Zawislak, B.; Virmani, A.; Schmued, L. L-carnitine and neuroprotection in the animal model of mitochondrial dysfunction. *Ann. N. Y. Acad. Sci.* **2005**, *1053*, 174–182.
22. Henique, C.; Mansouri, A.; Fumey, G.; Lenoir, V.; Girard, J.; Bouillaud, F.; Prip-Buus, C.; Cohen, I. Increased mitochondrial fatty acid oxidation is sufficient to protect skeletal muscle cells from palmitate-induced apoptosis. *J. Biol. Chem.* **2010**, *285*, 36818–36827.
23. Sayed-Ahmed, M.M.; Shouman, S.A.; Rezk, B.M.; Khalifa, M.H.; Osman, A.M.; El-Merzabani, M.M. Propionyl-L-carnitine as potential protective agent against adriamycin-induced impairment of fatty acid beta-oxidation in isolated heart mitochondria. *Pharmacol. Res.* **2000**, *41*, 143–150.
24. Myhill, S.; Booth, N.E.; McLaren-Howard, J. Chronic fatigue syndrome and mitochondrial dysfunction. *Int. J. Clin. Exp. Med.* **2009**, *2*, 1–16.
25. Pande, S.V.; Blanchaer, M.C. Reversible inhibition of mitochondrial adenosine diphosphate phosphorylation by long chain acyl coenzyme A esters. *J. Biol. Chem.* **1971**, *246*, 402–411.
26. Ramsay, R.R.; Zammit, V.A. Carnitine acyltransferases and their influence on CoA pools in health and disease. *Mol. Aspects Med.* **2004**, *25*, 475–493.
27. Zammit, V.A.; Ramsay, R.R.; Bonomini, M.; Arduini, A. Carnitine, mitochondrial function and therapy. *Adv. Drug Deliv. Rev.* **2009**, *61*, 1353–1362.
28. Iqbal, M.; Cawthon, D.; Wideman, R.F., Jr.; Bottje, W.G. Lung mitochondrial dysfunction in pulmonary hypertension syndrome I. Site-specific defects in the electron transport chain. *Poult. Sci.* **2001**, *80*, 485–495.
29. Kasahara, E.; Lin, L.R.; Ho, Y.S.; Reddy, V.N. SOD2 protects against oxidation-induced apoptosis in mouse retinal pigment epithelium: Implications for age-related macular degeneration. *Invest. Ophthalmol. Vis. Sci.* **2005**, *46*, 3426–3434.

30. Sharma, S.; Grobe, A.C.; Wiseman, D.A.; Kumar, S.; English, M.; Najwer, I.; Benavidez, E.; Oishi, P.; Azakie, A.; Fineman, J.R.; *et al.* Lung antioxidant enzymes are regulated by development and increased pulmonary blood flow. *Am. J. Physiol. Lung Cell. Mol. Physiol.* **2007**, *293*, L960–L971.
31. Fijalkowska, I.; Xu, W.; Comhair, S.A.; Janocha, A.J.; Mavrakis, L.A.; Krishnamachary, B.; Zhen, L.; Mao, T.; Richter, A.; Erzurum, S.C.; *et al.* Hypoxia inducible-factor1alpha regulates the metabolic shift of pulmonary hypertensive endothelial cells. *Am. J. Pathol.* **2010**, *176*, 1130–1138.
32. Fessel, J.P.; Hamid, R.; Wittmann, B.M.; Robinson, L.J.; Blackwell, T.; Tada, Y.; Tanabe, N.; Tatsumi, K.; Hemnes, A.R.; West, J.D. Metabolomic analysis of bone morphogenetic protein receptor type 2 mutations in human pulmonary endothelium reveals widespread metabolic reprogramming. *Pulm. Circ.* **2012**, *2*, 201–213.
33. Surmeli, N.B.; Litterman, N.K.; Miller, A.F.; Groves, J.T. Peroxynitrite Mediates Active Site Tyrosine Nitration in Manganese Superoxide Dismutase. Evidence of a Role for the Carbonate Radical Anion. *J. Am. Chem. Soc.* **2010**, *132*, 17174–17185.
34. Sener, G.; Paskaloglu, K.; Satiroglu, H.; Alican, I.; Kacmaz, A.; Sakarcan, A. L-carnitine ameliorates oxidative damage due to chronic renal failure in rats. *J. Cardiovasc. Pharmacol.* **2004**, *43*, 698–705.
35. Arafa, H.M.; Sayed-Ahmed, M.M. Protective role of carnitine esters against alcohol-induced gastric lesions in rats. *Pharmacol. Res.* **2003**, *48*, 285–290.
36. Aydogdu, N.; Atmaca, G.; Yalcin, O.; Taskiran, R.; Tastekin, E.; Kaymak, K. Protective effects of L-carnitine on myoglobinuric acute renal failure in rats. *Clin. Exp. Pharmacol. Physiol.* **2006**, *33*, 119–124.
37. Chavez, M.D.; Lakshmanan, N.; Kavdia, M. Impact of superoxide dismutase on nitric oxide and peroxynitrite levels in the microcirculation—A computational model. *Conf. Proc. IEEE Eng. Med. Biol. Soc.* **2007**, *2007*, 1022–1026.
38. Quijano, C.; Hernandez-Saavedra, D.; Castro, L.; McCord, J.M.; Freeman, B.A.; Radi, R. Reaction of peroxynitrite with Mn-superoxide dismutase. Role of the metal center in decomposition kinetics and nitration. *J. Biol. Chem.* **2001**, *276*, 11631–11638.
39. Konduri, G.G.; Mattei, J. Role of oxidative phosphorylation and ATP release in mediating birth-related pulmonary vasodilation in fetal lambs. *Am. J. Physiol. Heart Circ. Physiol.* **2002**, *283*, H1600–H1608.
40. Sessa, W.C. eNOS at a glance. *J. Cell. Sci.* **2004**, *117*, 2427–2429.
41. Gratton, J.P.; Fontana, J.; O'Connor, D.S.; Garcia-Cardena, G.; McCabe, T.J.; Sessa, W.C. Reconstitution of an endothelial nitric-oxide synthase (eNOS), hsp90, and caveolin-1 complex *in vitro*. Evidence that hsp90 facilitates calmodulin stimulated displacement of eNOS from caveolin-1. *J. Biol. Chem.* **2000**, *275*, 22268–22272.
42. Vescovo, G.; Ravara, B.; Gobbo, V.; Sandri, M.; Angelini, A.; Della Barbera, M.; Dona, M.; Peluso, G.; Calvani, M.; Mosconi, L.; *et al.* L-Carnitine: A potential treatment for blocking apoptosis and preventing skeletal muscle myopathy in heart failure. *Am. J. Physiol. Cell. Physiol.* **2002**, *283*, C802–C810.
43. Gulcin, I. Antioxidant and antiradical activities of L-carnitine. *Life Sci.* **2006**, *78*, 803–811.

44. Arduini, A. Carnitine and its acyl esters as secondary antioxidants? *Am. Heart J.* **1992**, *123*, 1726–1727.
45. Iliceto, S.; Scrutinio, D.; Bruzzi, P.; D'Ambrosio, G.; Boni, L.; Di Biase, M.; Biasco, G.; Hugenholtz, P.G.; Rizzon, P. Effects of L-carnitine administration on left ventricular remodeling after acute anterior myocardial infarction: The L-Carnitine Ecocardiografia Digitalizzata Infarto Miocardico (CEDIM) Trial. *J. Am. Coll. Cardiol.* **1995**, *26*, 380–387.
46. Aliev, G.; Liu, J.; Shenk, J.C.; Fischbach, K.; Pacheco, G.J.; Chen, S.G.; Obrenovich, M.E.; Ward, W.F.; Richardson, A.G.; Smith, M.A.; *et al.* Neuronal mitochondrial amelioration by feeding acetyl-L-carnitine and lipoic acid to aged rats. *J. Cell. Mol. Med.* **2009**, *13*, 320–333.
47. Abdul, H.M.; Calabrese, V.; Calvani, M.; Butterfield, D.A. Acetyl-L-carnitine-induced up-regulation of heat shock proteins protects cortical neurons against amyloid-beta peptide 1–42-mediated oxidative stress and neurotoxicity: Implications for Alzheimer's disease. *J. Neurosci. Res.* **2006**, *84*, 398–408.
48. Miguel-Carrasco, J.L.; Mate, A.; Monserrat, M.T.; Arias, J.L.; Aramburu, O.; Vazquez, C.M. The role of inflammatory markers in the cardioprotective effect of L-carnitine in L-NAME-induced hypertension. *Am. J. Hypertens.* **2008**, *21*, 1231–1237.
49. Pauly, D.F.; Pepine, C.J. The role of carnitine in myocardial dysfunction. *Am. J. Kidney Dis.* **2003**, *41*, S35–S43.
50. Tarantini, G.; Scrutinio, D.; Bruzzi, P.; Boni, L.; Rizzon, P.; Iliceto, S. Metabolic treatment with L-carnitine in acute anterior ST segment elevation myocardial infarction. A randomized controlled trial. *Cardiology* **2006**, *106*, 215–223.
51. Herrera, M.D.; Bueno, R.; de Sotomayor, M.A.; Perez-Guerrero, C.; Vazquez, C.M.; Marhuenda, E. Endothelium-dependent vasorelaxation induced by L-carnitine in isolated aorta from normotensive and hypertensive rats. *J. Pharm. Pharmacol.* **2002**, *54*, 1423–1427.
52. Bueno, R.; Alvarez de Sotomayor, M.; Perez-Guerrero, C.; Gomez-Amores, L.; Vazquez, C.M.; Herrera, M.D. L-carnitine and propionyl-L-carnitine improve endothelial dysfunction in spontaneously hypertensive rats: Different participation of NO and COX-products. *Life Sci.* **2005**, *77*, 2082–2097.
53. Wedgwood, S.; Black, S.M. Endothelin-1 decreases endothelial NOS expression and activity through ETA receptor-mediated generation of hydrogen peroxide. *Am. J. Physiol. Lung Cell. Mol. Physiol.* **2005**, *288*, L480–L487.
54. Song, P.; Wu, Y.; Xu, J.; Xie, Z.; Dong, Y.; Zhang, M.; Zou, M.H. Reactive nitrogen species induced by hyperglycemia suppresses Akt signaling and triggers apoptosis by upregulating phosphatase PTEN (phosphatase and tensin homologue deleted on chromosome 10) in an LKB1-dependent manner. *Circulation* **2007**, *116*, 1585–1595.
55. Black, S.M.; Bekker, J.M.; Johengen, M.J.; Parry, A.J.; Soifer, S.J.; Fineman, J.R. Altered regulation of the ET-1 cascade in lambs with increased pulmonary blood flow and pulmonary hypertension. *Pediatr. Res.* **2000**, *47*, 97–106.
56. McMullan, D.M.; Bekker, J.M.; Johengen, M.J.; Hendricks-Munoz, K.; Gerrets, R.; Black, S.M.; Fineman, J.R. Inhaled nitric oxide-induced rebound pulmonary hypertension: Role for endothelin-1. *Am. J. Physiol. Heart Circ. Physiol.* **2001**, *280*, H777–H785.

57. Wedgwood, S.; McMullan, D.M.; Bekker, J.M.; Fineman, J.R.; Black, S.M. Role for endothelin-1-induced superoxide and peroxynitrite production in rebound pulmonary hypertension associated with inhaled nitric oxide therapy. *Circ. Res.* **2001**, *89*, 357–364.
58. Sud, N.; Wells, S.M.; Sharma, S.; Wiseman, D.A.; Wilham, J.; Black, S.M. Asymmetric dimethylarginine inhibits HSP90 activity in pulmonary arterial endothelial cells: Role of mitochondrial dysfunction. *Am. J. Physiol. Cell. Physiol.* **2008**, *294*, C1407–C1418.
59. Kumar, S.; Sud, N.; Fonseca, F.V.; Hou, Y.; Black, S.M. Shear stress stimulates nitric oxide signaling in pulmonary arterial endothelial cells via a reduction in catalase activity: Role of protein kinase C delta. *Am. J. Physiol. Lung Cell. Mol. Physiol.* **2010**, *298*, L105–L116.
60. Laurindo, F.R.; Pedro Mde, A.; Barbeiro, H.V.; Pileggi, F.; Carvalho, M.H.; Augusto, O.; da Luz, P.L. Vascular free radical release *ex vivo* and *in vivo* evidence for a flow-dependent endothelial mechanism. *Circ. Res.* **1994**, *74*, 700–709.
61. Lakshminrusimha, S.; Wiseman, D.; Black, S.M.; Russell, J.A.; Gugino, S.F.; Oishi, P.; Steinhorn, R.H.; Fineman, J.R. The role of nitric oxide synthase-derived reactive oxygen species in the altered relaxation of pulmonary arteries from lambs with increased pulmonary blood flow. *Am. J. Physiol. Heart Circ. Physiol.* **2007**, *293*, H1491–H1497.
62. Black, S.M.; Heidersbach, R.S.; McMullan, D.M.; Bekker, J.M.; Johengen, M.J.; Fineman, J.R. Inhaled nitric oxide inhibits NOS activity in lambs: Potential mechanism for rebound pulmonary hypertension. *Am. J. Physiol.* **1999**, *277*, H1849–H1856.
63. McMullan, D.M.; Bekker, J.M.; Parry, A.J.; Johengen, M.J.; Kon, A.; Heidersbach, R.S.; Black, S.M.; Fineman, J.R. Alterations in endogenous nitric oxide production after cardiopulmonary bypass in lambs with normal and increased pulmonary blood flow. *Circulation* **2000**, *102*, III172–III178.

© 2013 by the authors; licensee MDPI, Basel, Switzerland. This article is an open access article distributed under the terms and conditions of the Creative Commons Attribution license (<http://creativecommons.org/licenses/by/3.0/>).